



Mode localization in composite laminates

Divyendu Sharma^a, S.S. Gupta^{b,*}, R.C. Batra^c

^a Department of Navy, Defence Institute of Advanced Technology, Girinagar, Pune 411 025, India

^b Department of Mechanical Engineering, Indian Institute of Technology Kanpur, Kanpur 208 016, India

^c Department of Engineering Science and Mechanics, M/C 0219, Virginia Polytechnic Institute and State University, Blacksburg, VA 24061, USA

ARTICLE INFO

Article history:

Available online 7 March 2012

Keywords:

Free vibration
Mode localization
Composite laminates
Vibration suppression

ABSTRACT

We study free vibrations of monolithic and composite thin rectangular plates; the former are made of linear elastic, homogeneous, isotropic materials and the latter of fiber reinforced laminas. The plates are clamped on all four edges and interior points on a transverse normal to the plate midsurface are rigidly tied together and have either null displacements and null rotations (Type-I constraint) or only null transverse displacements (Type-II constraint). Depending upon the location of the point on the midsurface through which the transverse normal passes, modes localize in different regions of the plate. Plates of various aspect ratios (length/width) and stacking sequences of 0°, 45° and 90° leading to symmetric and anti-symmetric configurations about their midsurfaces are considered. The problem is studied using the first order shear deformable (or the Mindlin) plate theory. It is found that both the Type-I and Type-II constraints divide the plate into two vibrating regions with amplitudes of transverse vibration localized in a particular region on either side of the clamped interior points. It is found that the mode localization in laminates is governed by the mode localization characteristics of constituent laminas. For symmetric cross ply laminates the localization of modes is found to decrease with the increase in the number of 0° plies. For anti-symmetric cross ply laminates and those made of all 45° plies the mode localization is found to be independent of the number of plies. For isotropic plates made of a monolithic material the mode localization phenomenon is stronger for Type-I constraint compared to that for Type-II constraints. Also, for these plates the mode localization occurs when lumped masses are placed at these interior points. The significance of the work lies in providing an alternative and an economical way of annulling plate vibrations in selected parts of the plate, and confining the energy of vibration in desired regions of the plate.

© 2012 Elsevier Ltd. All rights reserved.

1. Introduction

Much after the discovery of the phenomenon of localization in random crystal lattices by Anderson [1], many research groups have investigated the presence of mode localization or confinement of energy of vibration in a localized region in mechanical systems. The phenomenon of mode localization in mechanical systems is attributed to one or more of the following: randomness, disorder and irregularity in the periodicity of system parameters or boundary conditions. The system parameters could be mass or stiffness. The phenomenon of mode localization is characterized by almost an exponential decay of amplitude of vibration away from the driving point. The available literature on mode localization in mechanical systems can be divided into four different classes; (I) one-dimensional periodic, (II) cyclic symmetric, (III) two-dimensional periodic, and (IV) two-dimensional finite continuum.

A brief discussion of the literature pertaining to mode localization is presented below according to the above classification.

Using the theory of transmission and reflection of waves Hodges [2] qualitatively showed the phenomenon of mode localization in a straight long chain of regularly placed pendulums and in an infinitely long string supported on identical spring-mass systems at irregular intervals. In the example of chain of pendulums, the pendulums were weakly coupled to their neighbors on either side with identical springs. The irregularity was introduced by considering pendulums of different lengths whereas in the example of string, irregularity was introduced in the periodicity of supporting spring-mass systems. Hodges and Woodhouse [3] presented a theoretical framework and performed experiments on a string attached with lumped masses at irregular spacing to demonstrate mode localization. Pierre and Dowell [4] developed a perturbation method to study the mode localization in the system of irregularly coupled pendulums similar to the one studied by Hodges [2]. Their method considers small variations in system parameters and small coupling among subsystems as perturbations. Pierre et al. [5] extended the perturbation method developed in Ref. [4] to study

* Corresponding author.

E-mail address: ssgupta@iitk.ac.in (S.S. Gupta).

mode localization in a simply supported two span beam with a torsional spring at an intermediate point support. They found that the mode localization depends on the irregular spacing between the supports and the stiffness of the torsional spring, and theoretical results from the perturbation method agreed well with the experimental findings. Luongo [6] studied axial oscillations in clamped–clamped and clamped–free beams connected to regularly placed springs active in the axial direction. Then, by introducing periodic and aperiodic imperfections in the stiffness of springs, Luongo [6] showed the occurrence of mode localization.

Pierre and Plaut [7] studied the buckling of a simply supported two span beam with a torsional spring at an intermediate roller support. Using perturbation analysis they found mode localization for weak coupling between spans. The disorder was created by introducing slight irregular spacing between the supports. They concluded that the loci of the first two critical loads as a function of disorder are far separated for strong coupling and are very close to each other for weak coupling between the spans. This phenomenon of eigenvalue loci veering in buckling is similar to that reported by Pierre [8] in vibration problems. Nayfeh and Hawwa [9] extended Pierre and Plaut's work [7] and showed that the irregularity in spans of a column can be exploited to control its buckling using mode localization. Spletzer et al. [10] have used mode localization to increase the sensitivity of coupled micro-cantilevers made of gold to detect foreign particles. They showed that the conventional method of detecting a shift in the natural frequency of a single cantilever sensor due to added mass is much less sensitive than detecting the change in the mode shape due to localization in a coupled cantilever sensor. The disorder in the system was introduced by attaching a microsphere of borosilicate at the free end of one of the cantilevers. Thiruvengatathan et al. [11,12] extended Spletzer et al.'s [10] work to enhance the sensitivity of micro-electro-mechanical system (MEMS) based sensors. They used capacitive type electrical coupling to weaken the mechanical coupling in nearly identical double-ended tuning forks to increase the mode localization leading to enhanced sensitivity of sensors.

Bendiksen [13] studied the mode localization in a disordered and imperfect cyclic symmetric structure made of cantilever beams fixed on a hub with end masses (a model of wrap-rib dish antenna for space application) using a perturbation method. Bendiksen [13] suggested that the presence of imperfection and disorder in construction of large space antenna may adversely affect the performance of shape and direction control. Ottarsson and Pierre [14], and Xie and Ariaratnam [15] have used a transfer matrix approach to study mode localization in mistuned blade assembly and wrap-rib dish antenna, respectively.

Xie and Wang [16] used perturbation method to study localization in randomly ordered weakly coupled rectangular two-dimensional cantilever-spring arrays. The free ends of vertical cantilevers were connected to their nearest neighbors' free ends using eight springs in the horizontal plane, four in mutually perpendicular directions and other four in diagonal directions. They found that the strong localization takes place in the diagonal direction. Cai et al. [17] studied a bi-periodic rectangular two-dimensional array of spring-mass systems. The arrangement of spring-mass systems in their study is similar to that adopted by Xie and Wang [16], except that the cantilevers have been replaced by springs. The masses are connected to each other by infinitely long strings in two orthogonal directions with different pretension in them, and a disorder is introduced by slightly changing the mass at the center of the array.

Li et al. [18] have studied vibrations of an axially compressed, rib stiffened rectangular simply supported plate made of a homogeneous, linear elastic, and isotropic material. In their study the ribs are placed perpendicular to the long dimension of the plate and their spacing is assumed to be a uniformly distributed random

variable. Using transfer matrix approach they found that the localization increases with the increase in the randomness of placement of ribs. Using a finite strip method and the Galerkin projection Chen and Xie [19] studied free and forced vibration of a rectangular plate with two slightly misplaced orthogonal rib-stiffeners. In the ideal condition these stiffeners would divide the plate into four equal rectangles. The plate is considered to be made of a homogeneous, linear elastic and isotropic material. They found that the flexural rigidity and the misplacement of stiffeners influence the mode localization more than the torsional stiffness. Using a harmonic point force in a quadrant of the plate Chen and Xie [19] showed that during the resonance of a particular mode the response of the plate is the same as the mode localization of the resonant mode. Using the Kirchhoff plate theory Filoche and Mayboroda [20] studied mode localization in thin clamped rectangular plates of various aspect ratios (length/width) made of homogeneous, linear elastic and isotropic material having fixed points on the line bisecting the width and perpendicular to it. Using the finite element method (FEM) they computed several modes of transverse oscillations and found enhanced mode localization with an increase in the plate aspect ratio.

We have found that the available literature on mode localization in composite laminas and laminates is sparse. Plates/laminates are widely used structural elements in automobile, aircraft, naval and air-conditioning systems and one of the goals while designing these systems is to minimize transverse vibrations of constituent plate structures for reducing structural borne noise and fatigue failures. The phenomenon of mode localization offers an alternative method of controlling vibrations of flexible plates at lower cost as compared to constrained layer damping (CLD) treatment [21], active mechanisms [22–24] or hybrid mechanisms [25–27].

Here we generalize the work on mode localization for isotropic Kirchhoff plates reported in [20] to anisotropic composite thin shear deformable laminates. We use the FEM to find the first 100 modes of transverse vibration of laminates of various aspect ratios, different fiber orientations, stacking sequences, and the number of plies, and delineate effects of these variables on the mode localization.

The remainder of the paper is organized as follows. The procedure and the material properties used in the present study are explained in Section 2. The phenomenon of mode localization in an isotropic plate is discussed in Section 3. Section 4 describes the localization studies pertaining to composite laminas, and laminates, and conclusions of this work are summarized in Section 5. As mentioned in the abstract, the mode localization is studied for two cases, namely, when plate points on a transverse normal are clamped, the Type-I constraint, and when only transverse displacements of these points are zero, the Type-II constraint. In the former case, all five degrees of freedom of these points on the transverse normal are set equal to zero, and in the latter case only one degree of freedom equals zero. The stipulated boundary conditions at points on the transverse normal can be attained by using two rigid rods with a pointed edge on one side; the pointed ends support the plate from the opposite sides while the other ends of the rods are held against immovable supports. Thus the line passing through the two rods is normal to the plate midsurface.

2. Procedure

The geometric parameters of laminates studied here are shown in Fig. 1. The length and the width of plates are chosen such that their surface area is unity [20]. The aspect ratio of a laminate is varied by changing the eccentricity e shown in Fig. 1. The fiber orientation within laminates is defined by the local rectangular Cartesian coordinate system oxy with the x -axis making a positive

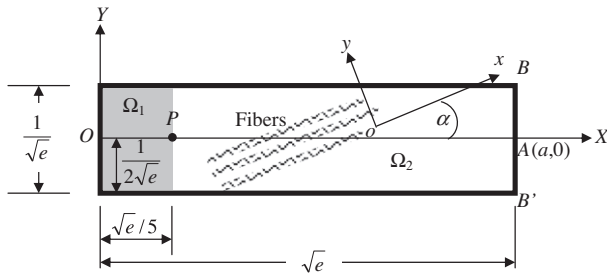


Fig. 1. Schematic of a lamina depicting geometric parameters, the location of the interior point P on the plate midsurface, fiber orientation, and regions Ω_1 (shaded) and Ω_2 where modes get localized after fixing points on the vertical line passing through point P . Clamped boundary conditions are prescribed on thick edges.

angle α measured counter-clockwise with the positive X -axis of the global rectangular Cartesian coordinate system OXY . We use the Mindlin (or the first order shear deformable) plate theory to study plate's deformations and employ the FEM with the midsurface discretized into 4-node quadrilateral elements. Each node has five degrees-of-freedom (DOF); u : the displacement along the X -axis, v : the displacement along the Y -axis, w : the displacement along the Z -axis, ϕ_x : the rotation about the X -axis and ϕ_y : the rotation about the Y -axis. The shear correction factor of $5/6$ is used to compute the plate stiffness matrix. The natural frequencies (eigenvalues) and the corresponding modes (eigenvectors) are obtained by solving the following equation of motion:

$$[M]\{\ddot{\delta}\} + [K]\{\delta\} = \{0\} \quad (1)$$

where $[M]$ and $[K]$ are the mass and the stiffness matrices, respectively, $\{\delta\}$ is the vector of active degrees of freedom, and a superimposed dot indicates the derivative with respect to time. The progressive mesh refinement process yielded $\sim 1\%$ difference between frequencies of first 100 out-of-plane (i.e., bending) modes computed with 18×200 (along the width and the length directions, respectively) and 20×240 FE meshes having uniform elements. Therefore, for all problems studied here the 20×240 FE mesh is used. The modes are *normalized* with respect to the mass matrix. The element stiffness matrix for a thin plate is computed by using reduced integration (one-point for the shear contribution and 2×2 Gauss integration rule for the bending contribution) in the thickness direction to avoid shear locking. At a clamped node on an edge values of all five DOFs are set equal to zero. For an interior point either values of all five DOFs are set to zero to simulate Type-I or only the w -DOF is set to zero to apply Type-II constraint. To study the effect of mass lumping on mode localization a fraction of total mass of the plate is added at the appropriate locations in the mass matrix. For these computations a code has been developed using MATLAB [28]. The code has been verified by comparing in Tables 1 and 2 the fundamental frequency of free vibration of simply supported cross-ply and angle-ply laminates with those available in the literature. The nondimensional frequency ($\bar{\omega}$) is computed from the relation $\bar{\omega} = (\omega e/h) \sqrt{\rho/E_2}$, where ω is the dimensional fundamental circular frequency, e is the square of the laminate length (e.g., see Fig. 1), h is the laminate thickness, ρ is the mass density, and E_2 is the elastic modulus in the direction perpendicular to the fiber axis. It is found that frequencies computed for various lay-ups of composite laminates using the code agree well with those reported by various research groups.

Using the verified MATLAB code, modes of vibration for clamped isotropic plates and composite laminates of various eccentricities are computed for Type I and Type II constraint conditions at interior point P (see Fig. 1). Furthermore, the effect of mass loading at point P is studied for isotropic plates. The location of

Table 1

Nondimensional fundamental frequency $\bar{\omega}$ for a simply supported square anti-symmetric cross-ply laminate with $a/h = 5$, $E_1/E_2 =$ either 20 or 30, $G_{12} = G_{13} = 0.6E_2$, $G_{23} = 0.5E_2$, $\nu_{12} = 0.25$.

Lamination scheme and number of layers	Source	E_1/E_2		
		20	30	
$(0^\circ, 90^\circ)_1$	Noor [29]	7.6745	8.1763	
	Whitney and Pagano [30]	7.6922	8.3112	
	Reddy [31]	7.8210	8.5050	
	Senthilnathan et al. [32]	7.8210	8.5050	
	Kant and Swaminathan [33] M1	7.7140	8.2775	
	Kant and Swaminathan [33] M2	7.6883	8.2570	
	Present	7.7230	8.3356	
	$(0^\circ, 90^\circ)_2$	Noor [29]	9.4055	10.1650
		Whitney and Pagano [30]	9.6729	10.6095
		Reddy [31]	9.6265	10.5348
Senthilnathan et al. [32]		9.6265	10.5348	
Kant and Swaminathan [33] M1		9.4675	10.2733	
Kant and Swaminathan [33] M2		9.4338	10.2463	
Present		9.6673	10.5894	

M1 and M2 are two different models.

point P does not affect the occurrence of the phenomenon of mode localization [20]. Following Filoche and Mayboroda [20] we select location of the interior point P as shown in Fig. 1.

2.1. Material properties

Material properties used in the present study are as follows:

Material-1: For the isotropic plate; $E_1 = E_2 = 210$ GPa, $\nu = 0.3$, $\rho = 8750$ kg/m³.

Material-2: For the composite lamina; $E_1 = 140$ GPa, $E_1/E_2 = 25$, $G_{12} = G_{13} = 2.8$ GPa, $G_{23} = 1.12$ GPa, $\nu_{12} = 0.25$, $\rho = 1600$ kg/m³.

Table 2

Nondimensional fundamental frequency $\bar{\omega}$ for a 10-layer simply supported angle-ply $(45^\circ/-45^\circ)_5$ square laminate with $E_1 = 15E_2$, $G_{12} = G_{13} = 0.5E_2$, $G_{23} = 0.35E_2$, $\nu_{12} = 0.3$.

a/h	Source	$\bar{\omega}$
5	Noor and Burton [34]	9.9825
	Reddy [35]	10.1537
	Whitney and Pagano [30]	10.1288
	Thai and Kim [36] M1	10.1537
	Thai and Kim [36] M2	10.1516
	Present	10.0958
10	Noor and Burton [34]	13.5100
	Reddy [35]	13.6078
	Whitney and Pagano [30]	13.6140
	Thai and Kim [36] M1	13.6078
	Thai and Kim [36] M2	13.6078
	Present	13.6019
100	Noor and Burton [34]	15.9500
	Reddy [35]	15.9482
	Whitney and Pagano [30]	15.9484
	Thai and Kim [36] M1	15.9482
	Thai and Kim [36] M2	15.9482
	Present	15.9662

M1 and M2 are two different models.

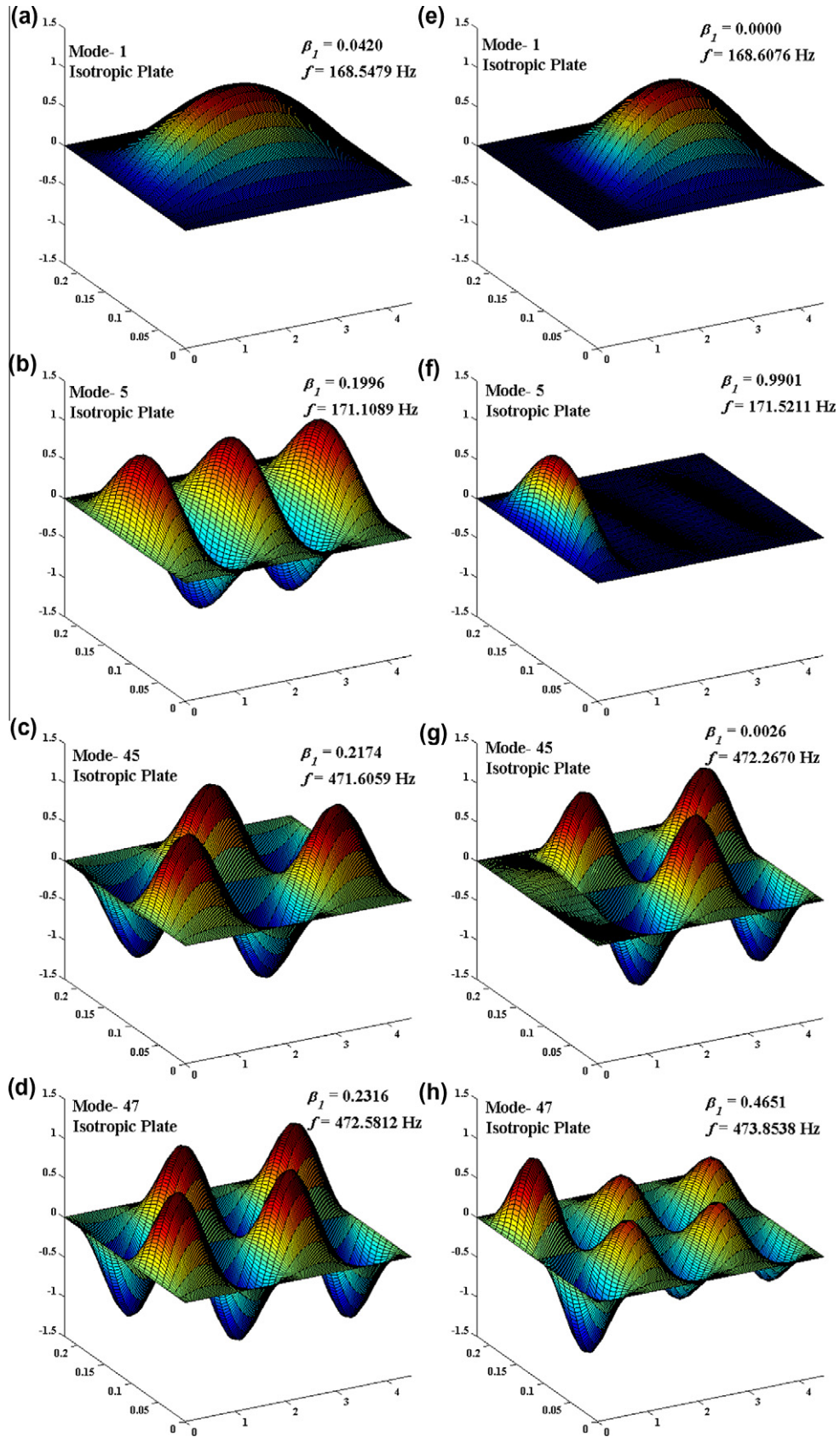


Fig. 2. Modes (mass normalized) of vibration of a clamped isotropic plate with $e = 20$. Modes in (a)–(d) correspond to the case when only edges of the plate are clamped and those in (e)–(h) correspond to the case when the interior point P (see Fig. 1) is also clamped.

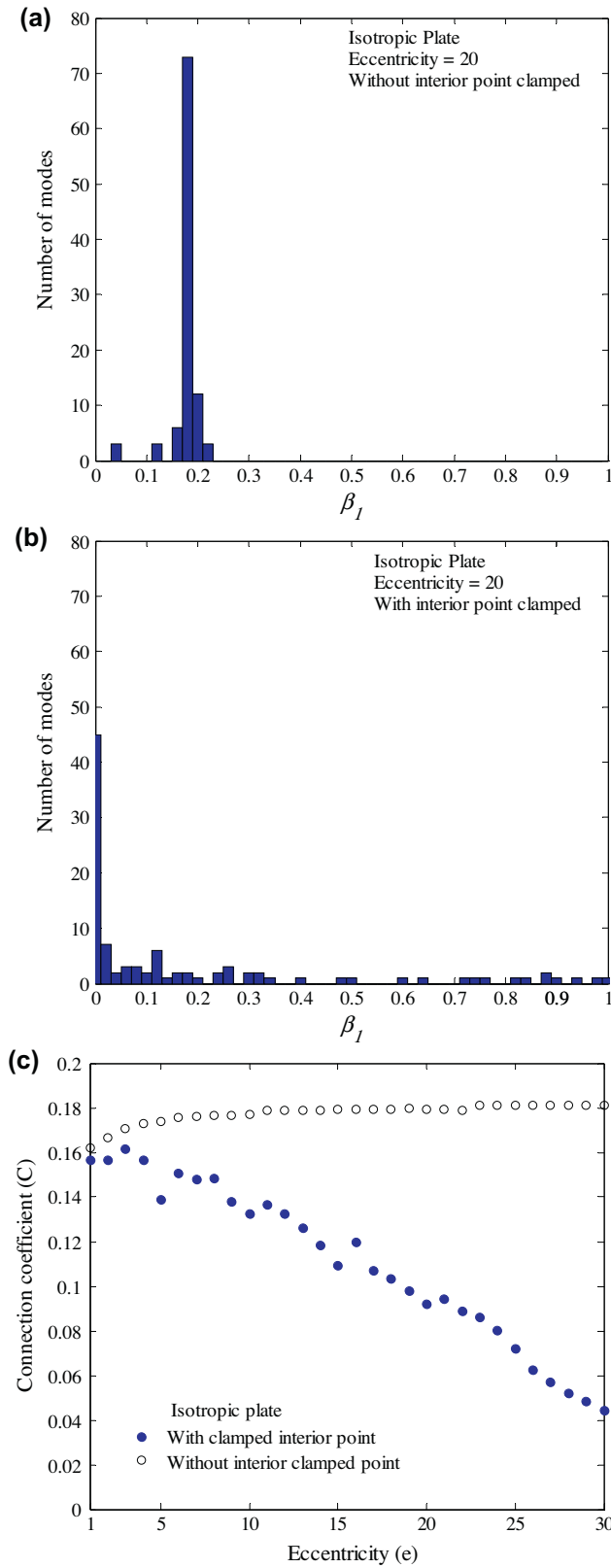


Fig. 3. Panels (a) and (b) show the distribution of β_1 for the first 100 out-of-plane modes of vibration of a plate made of an isotropic material without and with clamping an interior point, respectively. Panel (c) shows rapidly diminishing value of the connection coefficient with increasing eccentricity implying increased localization for higher values of eccentricity.

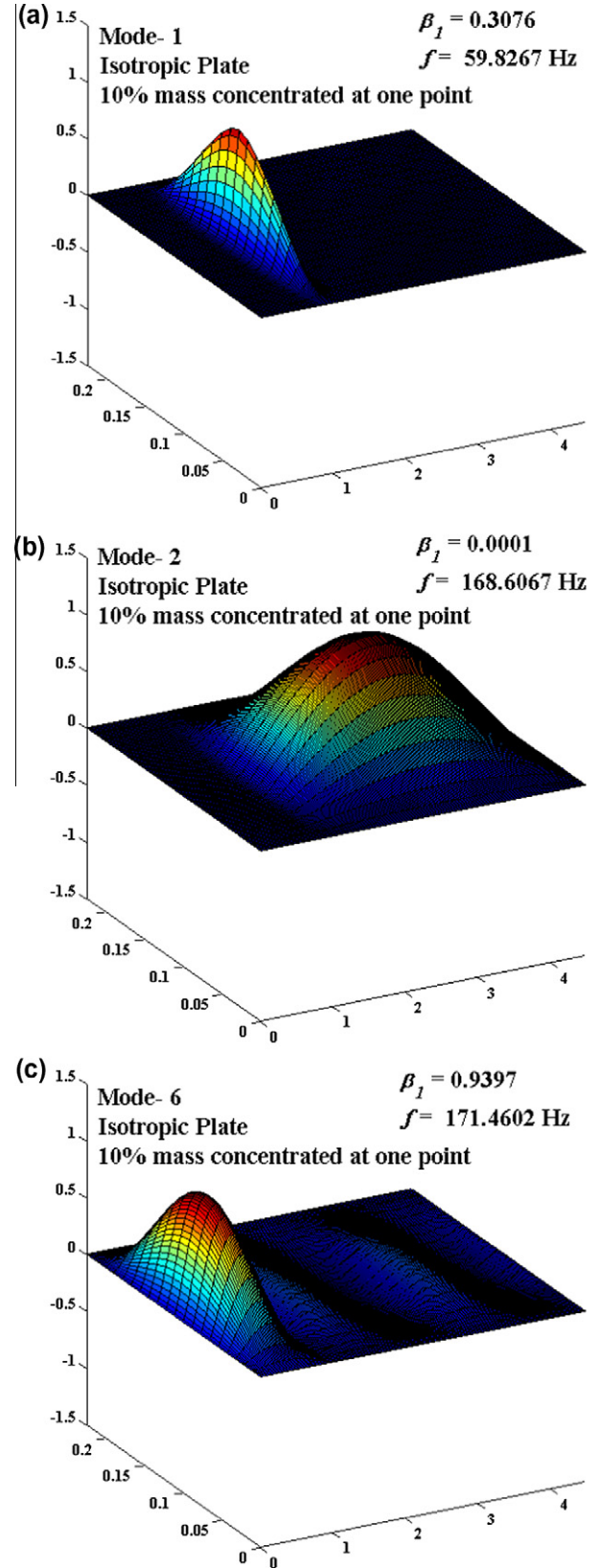


Fig. 4. Modes (mass normalized) of vibration of a clamped isotropic plate with eccentricity = 20. Modes in (a)–(c) correspond to the case when 10% of the total mass of the plate is added along the w degree-of-freedom of point P shown in Fig. 1.

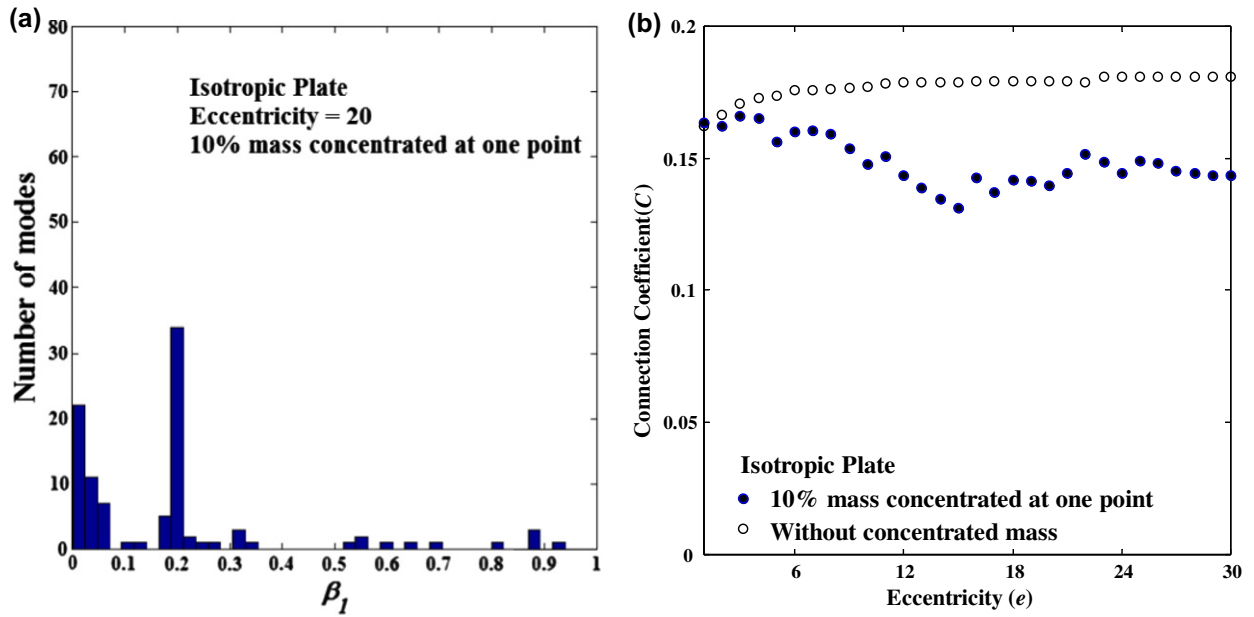


Fig. 5. Weak localization of modes of vibration in a plate made of an isotropic material when 10% of its total mass is added along the w-DOF of point P shown in Fig. 1. Panel (a) shows the distribution of β_1 for the first 100 transverse modes of vibration and Panel (b) shows the slowly diminishing value of C with increasing eccentricity.

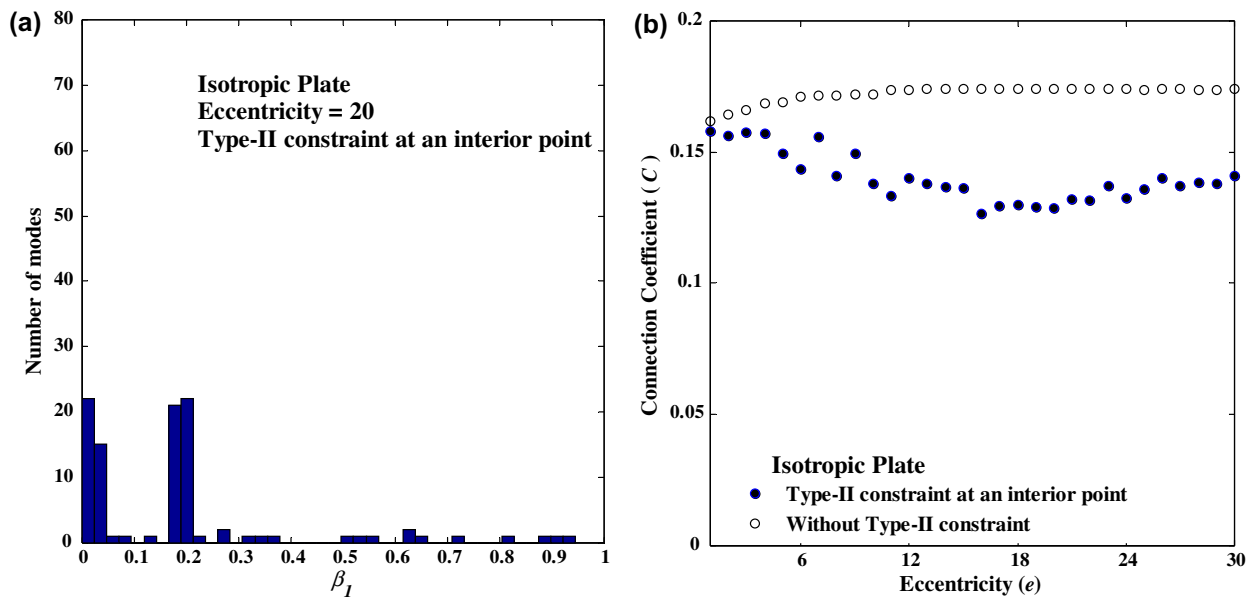


Fig. 6. Weak localization of modes of vibration in a plate made of an isotropic material when only the w-DOF of point P as shown in Fig. 1 is fixed. Panel (a) shows the distribution of β_1 for the first 100 transverse modes of vibration and Panel (b) shows the slowly diminishing value of C with increasing eccentricity.

3. Mode localization in isotropic and homogeneous plates

In this section we study mode localization in a clamped plate made of the linear elastic, homogeneous and isotropic material for Type-I and Type-II constraint conditions at an interior point, and when lumped mass is attached at an interior point. In the text which follows unless otherwise explicitly stated the clamped or fixed condition at an interior point implies Type-I constraint condition at that point.

The phenomenon of mode localization is shown in Fig. 2 for a plate with $e = 20$. It is seen from the deformed shapes plotted in Fig. 2e–h that fixing an interior point divides the plate into two

distinct regions Ω_1 and Ω_2 shown in Fig. 1; one in which the mode lives and the other in which the mode is completely/nearly silent. In Fig. 2, for the first mode the region Ω_1 is silent and for the fifth mode the region Ω_2 is silent. It may be noted that $\Omega = \Omega_1 \cup \Omega_2$. Let $\{o_1, o_2, \dots, o_n\}$ and $\{O_1, O_2, \dots, O_N\}$ be FEs contained in Ω_1 and Ω , respectively, and let $\{\delta\}_i, i = 1, 2, \dots, n$ and $\{\delta\}_j, j = 1, 2, \dots, N$ be vectors of DOF for nodes on elements o_i and O_j , respectively. We add that the FE mesh has nodes on the common boundary between regions Ω_1 and Ω_2 . Although various definitions have been used [37] to quantify mode localization, we use an energy based criterion and define a parameter β_1 by

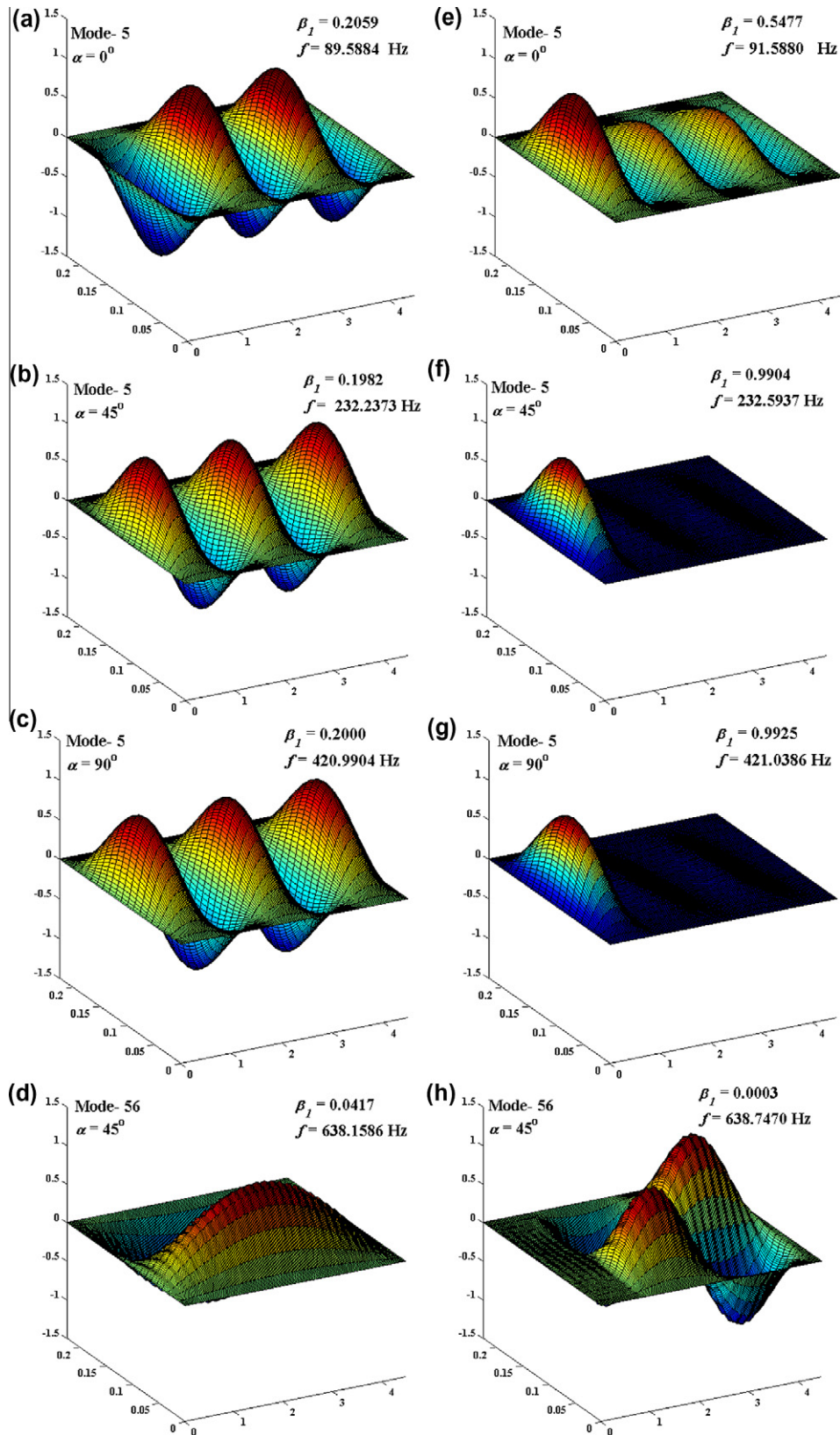


Fig. 7. Modes (mass normalized) of vibration of a clamped composite lamina with $e = 20$. Modes in (a)–(d) correspond to the case when only edges of the lamina are clamped and those in (e)–(h) correspond to the case when point P shown in Fig. 1 in the lamina interior is also clamped. For $\alpha = 45^\circ$, at higher frequency the half waves in the length direction of the lamina are oriented such that the nodal lines are inclined at 45° to the long side of the lamina. These length direction half waves superpose with the half waves along the width direction and produce ripples as shown in Panels (d) and (h).

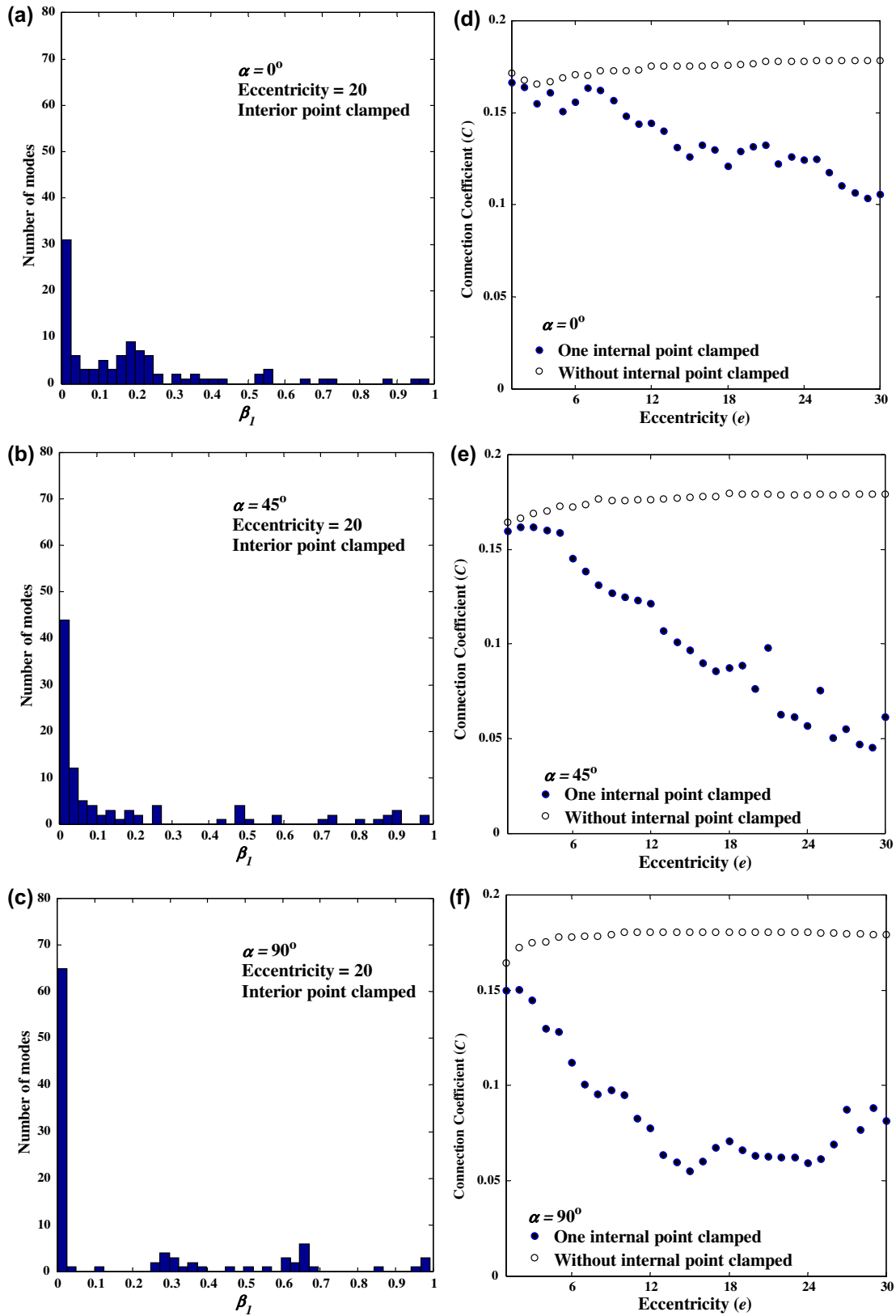


Fig. 8. Comparison of number of localized modes in a lamina for various fiber angles (Panels (a)–(c)) for $e = 20$. For 90° fiber orientation maximum number of modes are localized followed by 45° and 0° fiber orientation laminas. Variation of connection coefficient with eccentricity (Panels (d)–(f)).

$$\beta_1 = \frac{\sum_{i=1}^n \{\delta\}_i^T [k]_{el} \{\delta\}_i}{\sum_{j=1}^N \{\delta\}_j^T [k]_{el} \{\delta\}_j} \quad (2)$$

where $[k]_{el}$ is the stiffness matrix for element el that includes the shear correction factor. It is found that for clamped plates without any constraint at an interior point for most modes (with number

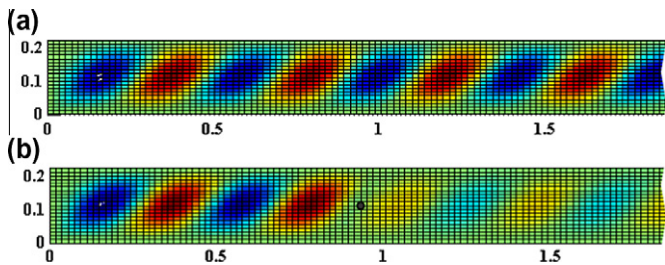


Fig. 9. (a) Mode-21 on a segment of a 45° lamina ($e = 20$) which is clamped on all sides and (b) the localized Mode-21 when an interior point (shown as a black dot) is also clamped. It is evident that the nodal lines are inclined at 45° to the long side of the lamina.

of half waves ≥ 2 along the long and the short sides of the plate, e.g. see Fig. 2b–d) the value of β_1 is proportional to the surface area of Ω_1 , which in the present case is 1/5. It is further noted from Fig. 2 that natural frequencies of vibration of the plate before and after clamping an interior point approximately remain the same; however, modes are changed significantly. For the isotropic plate having $e = 20$ without clamping an interior point, values of β_1 over the first 100 transverse modes are shown using the histogram in Fig. 3a. Fig. 3b shows that after clamping the interior point P most modes live in region Ω_2 ($\beta_1 \sim 0$). Also, there are significant number of modes with $0.0 < \beta_1 < 0.3$ implying moderate localization. A similar observation was made by Filoche and Mayboroda [20]. The dependence of mode localization on the eccentricity (aspect ratio) of a plate/lamina is quantified using a parameter called connection coefficient C [20] defined by

$$C = \frac{1}{S} \sum_{j=1}^{S=100} \min\{\beta_1, \beta_2\}_j \quad (3)$$

where S is the number of transverse modes of vibration of a plate/lamina. The value of C tending to zero implies the confinement of modes in either region Ω_1 or region Ω_2 . This further implies that the regions are disconnected in terms of the energy since parameters β_1 and $\beta_2 (= 1 - \beta_1)$ are obtained from Eq. (2). Without interior clamped points the variation in C with the eccentricity (see Fig. 3c) varying from 1 to 30 is found to be approximately constant and is expected to converge to 1/5 if a large number of transverse modes are considered for the plates. After clamping the interior points, it is found that the value of C decreases monotonically with an increase in the value of the eccentricity for the plates made of the same isotropic material. This agrees with Filoche and Mayboroda's [20] observation.

We have found that adding a small mass at the interior point P (see Fig. 1) rather than clamping it also induces mode localization. Fig. 4 shows modes with the lumped mass equal to 10% of the total mass of the plate added to point P . Interestingly, in the first mode (see Fig. 4a) the entire strain energy is localized in a very small region near point P and the frequency of this mode is significantly lower than that of the plate without the added lumped mass. Subsequent modes in the spectrum are similar to those shown in Fig. 2e and f. As shown in Fig. 5a the mode localization for the plate with the added lumped mass is not as strong as that in the plate with the interior clamped point for the eccentricity of 20. With the increase in the eccentricity from 0 to 15 the connection coefficient decreases slightly. For higher values of the eccentricity it increases slightly and then remains constant. According to this measure it is clear that the mode localization for all values of e is not as strong as that when point P is fixed. We have also studied the effect of two other values of lumped mass fractions viz. 5%

and 20% at point P and found similar behavior as that for the 10% lumped mass case.

For clamped plates with Type-II constraint at point P (that is, constraining only the w -DOF) the mode localization is found to be weak, see Fig. 6. This constraint is favorable for the formation of several standing waves along the length and the width directions with non-zero slope at P . This implies that at P , Type-II constraint is locally less stiff than that of the clamped constraint (i.e., Type-I constraint). The clamped constraint is favorable to only those standing waves that have zero slope at point P or satisfaction of the clamped constraint by a standing wave results in reduced amplitude in either region Ω_1 or region Ω_2 .

4. Mode localization in composite laminas/laminates

In this section the effect of fiber orientation, symmetry and anti-symmetry of lay-up, and the number of layers on mode localization in composite laminas and laminates is discussed. For these plates we have used values of elastic constants of material-2 listed above.

4.1. Mode localization in composite laminas

Before studying mode localization in laminates, we analyze the effect of fiber orientation on mode localization for a constituent lamina. For an arbitrarily chosen mode number, e.g., Mode-5, mode localization for 0°, 45° and 90° fiber orientation is shown in Fig. 7. As for an isotropic plate made of material-1, we find that natural frequencies of vibration of a lamina before and after clamping an interior point remain essentially unchanged but the modes are changed significantly. Fig. 8a–c shows the number of localized modes for $e = 20$. Furthermore, for each one of the three fiber orientations we note that the localized mode is the one which otherwise is the mode of the lamina when no interior point is clamped. In other words, we do not find any mode in the region Ω_1 which contains a standing wave with two half waves along the Y -axis while the region Ω_2 has standing waves with one half wave along the X -axis and vice versa. Since the bending stiffness $D_{11} = \sim 13D_{22}$ for $\theta = 0^\circ$ standing waves with higher half wave number along the Y -axis are formed at lower frequencies than those for $\theta = 90^\circ$ for which $D_{22} = \sim 13D_{11}$. This is why there are more modes with $\beta_1 \sim 0$ for the 90° lamina as compared to those in the 0° lamina when an interior point is clamped. Since $D_{11} = D_{22}$ for the 45° lamina nodal lines are inclined at 45° to the X -axis for higher frequencies (see Fig. 9) and the number of modes with $\beta_1 \sim 0$ is found to be between that for the 0° and the 90° laminas. Furthermore, we note that for the 0° and the 45° laminas there are several modes with $0 < \beta_1 < 0.3$ implying moderate localization of modes.

Variations of connection coefficient with eccentricity for the laminas studied herein are shown in Fig. 8d–f. We notice that for clamped laminas without an interior clamped point the value of C is approximately constant. As for the isotropic plates studied above, we expect the value of C to converge to 1/5 if a large number of transverse modes are considered. For the 0° and 45° laminas regions Ω_1 and Ω_2 increasingly become disconnected with the increase in the eccentricity. However, for the same eccentricity value the connection coefficient is found to be higher for the 0° lamina than that for the 45° lamina. Spikes in the value of C for some values of the eccentricity for the 45° lamina are due to the formation of higher half waves along the width direction. For the 90° lamina the value of C first decreases with the increase in the eccentricity up to $e = 15$ and for subsequent values of e it increases due to the formation of higher half waves along the width direction.

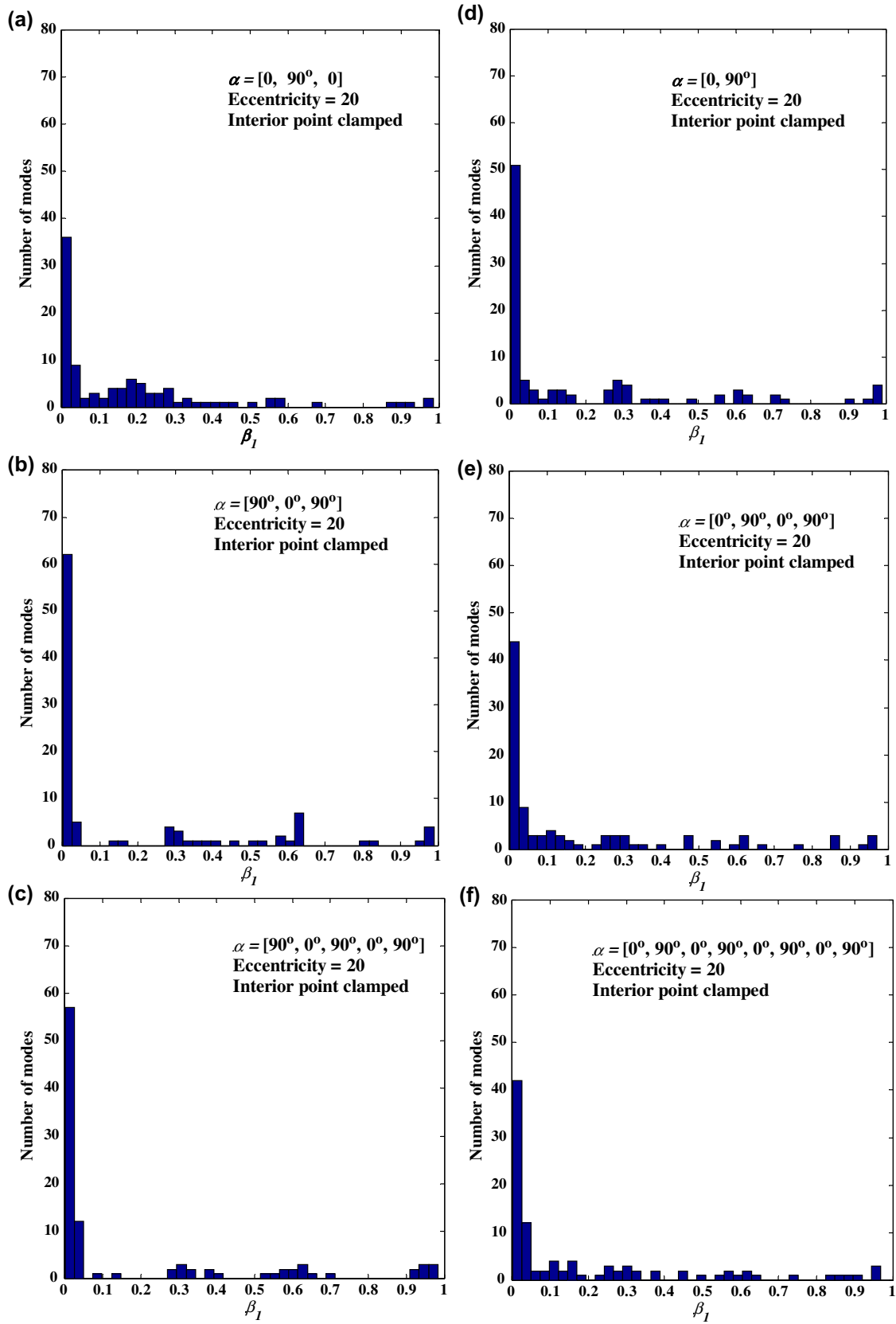


Fig. 10. Modal localization in symmetric (Panels (a)–(c)) and anti-symmetric (Panels (d)–(f)) cross-ply laminates of different number of layers for $e = 20$. The mode localization is found to decrease due to the presence of 0° layers and increase due to the presence of 90° layers.

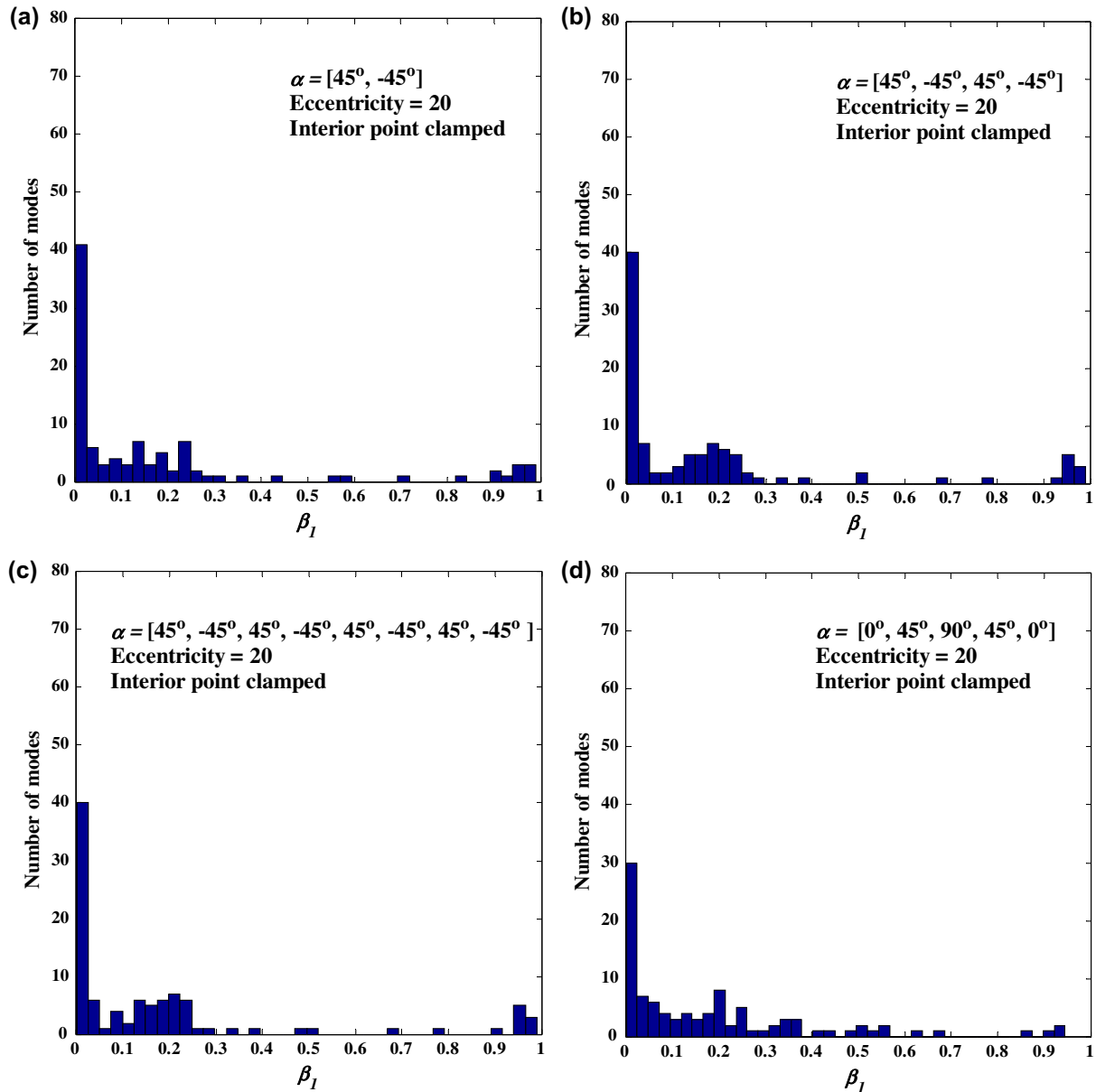


Fig. 11. Modal localization in anti-symmetric (Panels (a)–(c)) angle-ply laminates remains unaffected by the number of layers. Inclusion of 0° layers in a symmetric angle-ply laminate (Panel (d)) decreases the mode localization.

4.2. Mode localization in composite laminates

We have investigated mode localization in symmetric and anti-symmetric, cross-ply and angle-ply laminates made of constituent laminas studied above. It is found that the mode localization in a laminate is governed by the mode localization characteristics of the constituent laminas.

For symmetric cross-ply ($0^\circ/90^\circ/0^\circ$) and ($90^\circ/0^\circ/90^\circ$) laminates, the number of localized modes in region Ω_1 is more for the latter due to two 90° laminas (cf. Fig. 10a and b) or the number of localized modes in the same region is less in the former due to two 0° laminas. The addition of one 0° and one 90° lamina in ($90^\circ/0^\circ/90^\circ$) laminate does not significantly alter the mode localization; see Fig. 10c. From Fig. 10d–f, it is seen that in general anti-symmetric cross-ply laminates exhibit less mode localization than symmetric laminates. The number of localized modes is found to

decrease with the addition of a pair of 0° and 90° laminas in ($0^\circ/90^\circ$) laminate, however, adding more pairs of 0° and 90° laminas in ($0^\circ/90^\circ$) laminate do not. We have found that in going from ($0^\circ/90^\circ$)₁ \rightarrow ($0^\circ/90^\circ$)₂ \rightarrow ($0^\circ/90^\circ$)₃ \rightarrow ($0^\circ/90^\circ$)₄ the number of localized modes saturates to ~ 40 in region Ω_1 . For the sake of brevity we have omitted plots of distribution of the number of modes vs. β_1 for ($0^\circ/90^\circ$)₃ laminate. Furthermore, for symmetric cross-ply laminates with the number of 0° laminas more than the number of 90° laminas, and in general in anti-symmetric cross-ply laminates there are several modes with $0 < \beta_1 < 0.3$.

In anti-symmetric angle-ply laminates made of $\pm 45^\circ$ laminas it is found that the number of localized modes are unaffected by the number of layers as shown in Fig. 11a–c. The number of localized modes in these laminates is found to be ~ 40 . We have also studied an angle-ply symmetric laminate which contains all the constituent laminas characterized above. In this laminate fewer modes

than those in the cross-ply symmetric laminates localized primarily due to the presence of 0° plies. For all symmetric and anti-symmetric laminates studied there are several modes with $0 < \beta_1 < 0.3$.

5. Conclusions

By using the first order shear deformation theory we have analyzed mode localization in a clamped rectangular plate of various eccentricities with points on a transverse normal to the plate mid-surface either fully clamped (the Type-I constraint) or partially clamped (Type-II constraint). In the former case all five DOFs are set equal to zero, and in the latter case only the transverse displacement is set equal to zero. The plate material could be either linear elastic, homogeneous and isotropic or anisotropic fiber-reinforced composite with plies having fibers aligned at 0° , 45° or 90° . From the analysis of first 100 transverse modes of vibration it is found that the mode localization in isotropic plates and laminas of 45° and 90° fiber orientations is stronger than that in the 0° lamina. Mode localization in laminates is found to depend on the mode localization characteristics of the constituent laminas. For symmetric cross-ply laminates the presence of 0° ply reduces mode localization. Mode localization in anti-symmetric cross-ply and angle-ply laminates is found to be independent of the number of plies. Furthermore, for an isotropic plate adding mass to nodes on the transverse normal to the plate midsurface induces weak mode localization. Thus vibrations of a part of the plate can be controlled by either clamping points on a transverse normal or adding masses to points on the transverse normal passing through an interior point of the plate.

Acknowledgement

SSG's work was partially supported by Research Initiation Grant from IIT Kanpur. RCB's work was partially supported by the ONR grant N00014-11-1-0594 to Virginia Polytechnic Institute and State University.

References

- [1] Anderson PW. Absence of diffusion in certain random lattices. *Phys Rev* 1958;109(5):1492–505.
- [2] Hodges CH. Confinement of vibration by structural irregularity. *J Sound Vib* 1982;82(3):411–24.
- [3] Hodges CH, Woodhouse J. Vibration isolation from irregularity in a nearly periodic structure: theory and measurements. *J Acoust Soc Am* 1983;74(3):894–905.
- [4] Pierre C, Dowell EH. Localization of vibrations by structural irregularity. *J Sound Vib* 1987;114(3):549–64.
- [5] Pierre C, Tang DM, Dowell EH. Localized vibrations of disordered multispan beams: theory and experiment. *AIAA J* 1987;25(9):1249–57.
- [6] Luongo A. Mode localization by structural imperfections in one-dimensional continuous systems. *J Sound Vib* 1992;155(2):249–71.
- [7] Pierre C, Plaut RH. Curve veering and mode localization in buckling problem. *J Appl Math Phys* 1989;40:758–61.
- [8] Pierre C. Mode localization and eigenvalue loci veering phenomenon in disordered structures. *J Sound Vib* 1988;126(3):485–502.
- [9] Nayfeh AH, Hawwa MA. Use of mode localization in passive control of structural buckling. *AIAA J* 1994;32(10):2131–3.
- [10] Spletzer M, Raman A, Wu AQ, Xu X, Reifengerger R. Ultrasensitive mass sensing using mode localization in coupled microcantilevers. *Appl Phys Lett* 2006;88 [Art. No. 254102].
- [11] Thiruvankatanathan P, Yan J, Woodhouse J, Seshia AA. Enhancing parametric sensitivity in electrically coupled MEMS resonators. *J Microelectromech Syst* 2009;18(5):1077–86.
- [12] Thiruvankatanathan P, Yan J, Woodhouse J, Aziz A, Seshia AA. Ultrasensitive mode-localized mass sensor with electrically tunable parametric sensitivity. *Appl Phys Lett* 2010;96 [Art. No. 81913].
- [13] Bendiksen OO. Mode localization phenomenon in large space structures. *AIAA J* 1987;25(9):1241–8.
- [14] Ottarsson G, Pierre C. A transfer matrix approach to free vibration localization in mistuned blade assemblies. *J Sound Vib* 1996;197(5):589–618.
- [15] Xie WC, Ariaratnam ST. Vibration mode localization in disordered cyclic structures. I: single substructure mode. *J Sound Vib* 1996;189(5):625–45.
- [16] Xie WC, Wang X. Vibration mode localization in two-dimensional systems. *AIAA J* 1997;35(10):1653–9.
- [17] Cai CW, Liu JK, Yang Y. Exact analysis of localized modes in two-dimensional bi-periodic mass-spring systems with a single disorder. *J Sound Vib* 2005;288:307–20.
- [18] Li FM, Wang YS, Hu C, Huang WH. Localization of elastic waves in periodic rib-stiffened rectangular plates under axial compressive load. *J Sound Vib* 2005;281:261–73.
- [19] Chen Z, Xie W-C. Vibration localization in plates rib-stiffened in two orthogonal directions. *J Sound Vib* 2005;280:235–62.
- [20] Filoche M, Mayboroda S. Strong localization induced by one clamped point in thin plate vibrations. *Phys Rev Lett* 2009;103 [Art. No. 254301].
- [21] Yan M-J, Dowell EH. Governing equations for vibrating constrained layer damping sandwich plates and beams. *J Appl Mech* 1972;39(4):1041–6.
- [22] Clark RL, Fleming MR, Fuller CR. Piezoelectric actuators for distributed vibration excitation of thin plate: a comparison between theory and experiment. *J Vib Acoust* 1993;115:332–9.
- [23] Batra RC, Ghosh K. Deflection control during dynamic deformations of a rectangular plate using piezoceramic elements. *AIAA J* 1995;33:1547–8.
- [24] Gupta SS, Patel BP, Ganapathi M, Umopathy M, Bhawe SY. Non-linear dynamic analysis of laminated plates/shells with piezoelectric sensors and actuators. In: Proceedings of SPIE's symposium on smart materials, structures and MEMS, 11–14 December, 1996. Bangalore, India: Indian Institute of Science; 1996.
- [25] Baz A, Ro J. Optimum design and control of active constrained layer damping. *J Mech Des* 1995;117(B):135–44.
- [26] Huang SC, Inman DJ, Austin EM. Some design considerations for active and passive constrained layer damping treatments. *Smart Mater Struct* 1996;5(3):301–13.
- [27] Rongong JA, Wright JR, Wynne RJ, Tomlinson GR. Modeling of a hybrid constrained layer/piezoceramic approach to active damping. *J Vib Acoust* 1997;119:120–30.
- [28] User's manual 2005, MATLAB. The Math Works Inc., MA, USA.
- [29] Noor AK. Free vibrations of multilayered composite plates. *AIAA J* 1973;11:1038–9.
- [30] Whitney JM, Pagano NJ. Shear deformation in heterogeneous anisotropic plates. *ASME J Appl Mech* 1970;37(4):1031–6.
- [31] Reddy JN. A simple higher order theory for laminated composite plates. *ASME J Appl Mech* 1984;51:745–52.
- [32] Senthilnathan NR, Lim KH, Lee KH, Chow ST. Buckling of shear deformable plates. *AIAA J* 1987;25(9):1268–71.
- [33] Kant T, Swaminathan K. Analytical solutions for free vibration of laminated composite and sandwich plates based on a higher order refined theory. *Compos Struct* 2001;53(1):73–85.
- [34] Noor AK, Burton WS. Stress and free vibration analysis of multilayered composite plates. *Compos Struct* 1989;11(3):183–204.
- [35] Reddy JN. Mechanics of laminated composite plate theory and analysis. New York: CRC Press; 1997.
- [36] Thai HT, Kim SE. Free vibration of laminated composite plates using two variable refined plate theory. *Int J Mech Sci* 2010;52:626–33.
- [37] Visscher WM, Gubernatis JE. Computer experiments in disordered solids. In: Horton GK, Maradudin AA, editors. Dynamical properties of solids. Disordered solids, optical properties, vol. 4. Amsterdam: North-Holland Publishing Company; 1980.